



## DYNAMICS OF SOLITONS IN POLYACETYLENE IN THE STEP-POTENTIAL MODEL

Christoph Kuhn

Laboratoire Léon Brillouin, C.E. de Saclay, Bat. 563  
F-91191 Gif-Sur-Yvette Cedex, France

Wilfred F. van Gunsteren

Physikalische Chemie, Eidgenössische Technische Hochschule Zürich  
CH-8092 Zürich, Switzerland

(Received 4 May 1993 by M. Cardona)

In treating the motion of solitonic excitations in polyacetylene Newton's equation is used to approximate the lattice dynamics. The force field is obtained from the deviation of the  $\pi$ -electron densities in the bonds from their equilibrium densities. The  $\pi$ -electron density distributions are evaluated with the step-potential model. This model of a nearly free  $\pi$ -electron coupled to the elastic lattice of  $\sigma$ -bonded hydrocarbon ions is the conceptually simplest approach and has no free parameters. The electron-phonon coupling constant is scaled to butadiene and benzene. It is shown that a neutral kink moves frictionless for velocities up to three times the velocity of sound and shakes off phonons at higher velocities. This is in contrast to the results of the SSH-model, where the maximum velocity of the neutral kink is expected to be in a considerable range (0.6-4.0 times velocity of sound) depending on adjustable parameters.

### INTRODUCTION

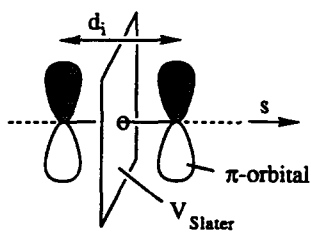
The problem of transmitting a signal through a  $\pi$ -electron system has been widely discussed [1,2]. Transport of solitons through a polyene chain within the (Su Schrieffer Heeger)-model was subject of a number of papers [6-11]. The lattice dynamics is usually treated in standard adiabatic approximation using Newton's equation of motion. The force required to integrate Newton's equation is usually obtained as the negative gradient of a potential energy surface. The equation of motion is integrated numerically using finite time steps. The result of the integration depends on the accuracy and stability of the algorithm used [12-16]. We have recently shown, that the statics [17] and dynamics [18, 19] of solitonic excitations can be treated by a simple step-potential model of a nearly free  $\pi$ -electron (NFE) coupled to the elastic lattice of  $\sigma$ -bonded hydro-carbon ions leading essentially to the same results as the (SSH)-model. However, the (SSH)-model calculations yield a maximum speed of the soliton depending strongly on adjustable parameters, while in our model the result (maximum speed of soliton being three times velocity of sound) is given by the strength of the electron-phonon coupling.

It is thus of interest to compare the physical implications of the (SSH-Hückel)-theory and the (NFE)-model and to shed the differences in structure of the models.

Both models have the same starting point: the many body  $\pi$ -electron Hamiltonian simplified to a Hamiltonian for independent electrons [20] moving in orbitals to be described as solutions of the Schrödinger equation of an electron in a potential  $V(x,y,z)$  associated with the  $\text{CH}^+$  lattice sites. These orbitals have nodes in the layer plane (orthogonality with  $\sigma$ -electrons). In both approaches  $V(x,y,z)$  is constructed from atomic contributions. The difference between the two approaches is given by the strategy of finding approximate solutions of that Schrödinger equation. In the refined free electron model, in contrast to the Hückel-LCAO and beyond, the Schrödinger equation for the molecular potential is numerically solved to obtain the eigen values and the corresponding orthonormal wave functions. The potential has been systematically simplified to investigate what features of  $V(x,y,z)$  are crucial to still describe main aspects of  $\pi$ -electron systems [21, 22]. In the case of chains with bonds fixed to equal bond length the most radical simplification of  $V(x,y,z)$  is the free electron model (orbitals where the factor depending on the coordinates perpendicular to the chain is the same for all  $\pi$ -electrons and the factor in the direction of the chain is a sine function corresponding to a constant potential). The step potential model using bond potentials being lower for the shorter bond is the logical extension of the free electron model in the case of chains with bonds fixed to unequal bond length. The value  $V_i$  of the potential step

corresponding to bond  $i$  is fixed to the averaged Slater potential from the two adjacent  $\text{CH}^+$  lattice sites taken in the middle of a bond (Fig. 1), i.e. the contribution of all  $\text{CH}^+$ -ions besides the next neighbours are neglected. The Coulomb charges of these ions are considered to be shielded by the residual  $\pi$ -electrons. In contrast, next neighbour ions are considered to be unshielded [23].

In the step potential model of a hydrocarbon chain of  $M$  bonds with unknown bond lengths  $d_1, d_2, \dots, d_M$  the  $\pi$ -electron is considered as an electron in a one dimensional potential composed of successive bond potentials  $V_1(d_1), V_2(d_2), \dots, V_M(d_M)$ , each bond potential being



$$\bar{V}_{\text{Slater}}(\text{in middle of bond } i) \longleftarrow \bar{V}_{\text{Slater}}(s) \\ = V_i(d_i)$$

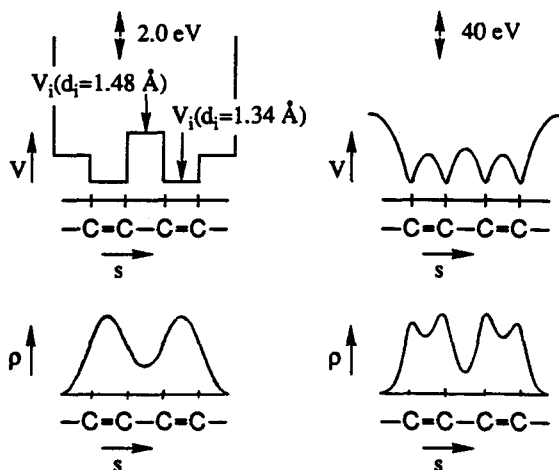


**Fig.1** The potential of a  $\pi$ -electron along the bond is approximated by the sum of atomic contributions from the two adjacent  $\text{CH}^+$  lattice sites. The one-dimensional model in the case of butadiene: Slater potential averaged perpendicular to the bond, as a function of  $s$  and the corresponding  $\pi$ -electron charge density distribution (right). Value  $V_i$  of the potential step corresponding to bond  $i$  of length  $d_i$  is fixed to the averaged Slater potential taken in the middle of the bond and the corresponding  $\pi$ -electron charge density distribution (left).

constant and of length  $a=1.40\text{\AA}$ . This Schrödinger equation is solved numerically and the wave functions are obtained as outlined in [17]. The lowest states are filled with the  $\pi$ -electrons present in the system and the  $\pi$ -electron density in the middle of each bond  $\rho_i(V_1, V_2, \dots, V_M)$  is obtained.

The  $\pi$ -electron charge in the bond  $i$  attracts the adjacent  $\sigma$ -bonded  $\text{CH}^+$ -ions by Coulomb forces and thus reduces the bond length  $d_i$  and the corresponding bond potential  $V_i(d_i)$ . The compression of bond  $i$  counteracts with the elastic forces caused by the Coulomb repulsion of the adjacent  $\text{CH}^+$ -ions and their attraction by the  $\sigma$ -electrons in between. This electron-phonon coupling is described within the step potential model by using the following relation between  $\rho_i$  and  $V_i$  iteratively:

$$V_i = \alpha (1 - \rho_i a) \frac{\hbar^2}{2ma^2}, \quad \alpha = 1.95 \quad (1)$$

( $\hbar^2/2ma^2 = 1.944 \text{ eV}$ ), where the strength of the electron-phonon coupling,  $\alpha$ , is scaled to the experimental bond lengths of butadiene and benzene. Applying equation (1) for each  $\rho_i$  and solving the Schrödinger equation for the new configuration of bond potentials initiates in return a cycle of an iteration, which converges to selfconsistency between  $\rho_i$  and  $V_i$  and thus finds the equilibrium density

$$\tilde{\rho}_i (\tilde{V}_1, \tilde{V}_2, \dots, \tilde{V}_M)$$

of bond  $i$  and all equilibrium bond lengths  $\tilde{d}_1, \tilde{d}_2, \dots, \tilde{d}_M$  of the relaxed molecular lattice of the hydrocarbon chain under consideration. All consequences follow unambiguously [17]: the absorption spectra and bond lengths of polyenes, polymethines and annulenes and the solitonic excitations in polyacetylene. The value  $\alpha=1.95$  in the equation (1) is unambiguously given.[23] A value  $\alpha>2.6$  would yield to bond length alternation in benzene. Therefore the resulting equal bonds in benzene and the transition from equal bonds to alternating bonds in the 18-annulene is not obvious but an important test for the model. This transition is reached within the (SSH)-model, searching for the energy minimum, by parameter fit [24].

## FORCE FIELD FOR THE DYNAMICS

The dynamics in standard adiabatic approximation follows from Newton's equation for every site  $i$ :

$$M_{\text{CH}} \cdot \frac{d^2}{dt^2} x_i = F_i \quad (2)$$

where  $x_i$  is the coordinate of site  $i$  representing a  $\text{CH}^+$  group with mass  $M_{\text{CH}} = 23888 m = 2.176 \cdot 10^{-26} \text{ kg}$ . The displacements are constrained to the molecular axis along  $x$  and thus  $d_i \sin \varphi_i = \frac{a}{2}$ , where  $d_i = \frac{x_{i+1} - x_i}{\cos \varphi_i}$  is the length of bond  $i$  (Fig. 2). The  $\sigma$ -bonds in the field of the  $\pi$ -electron cloud are compressed according to the

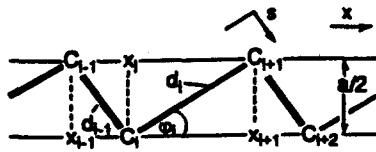


Fig.2 Zig-zag structure of polyacetylene along *s*. CH groups restricted to the track along *x*.

$\pi$ -electron density in each bond until the equilibrium configuration is reached. During dynamics the molecular lattice is not relaxed. Thus, in analogy to Hooke's law, the strain arising in bond *i* is proportional to the deviation  $\tilde{\rho}_i - \rho_i$  of the actual  $\pi$ -electron density  $\rho_i$  from the equilibrium density  $\tilde{\rho}_i$ . For small deviations of the actual density  $\rho_i$  from its equilibrium it is assumed that the equilibrium density  $\tilde{\rho}_i$  ( $\rho_1, \rho_2, \dots, \rho_M$ ) is obtained by applying equation (1) for each  $\rho_i$  and solving the Schrödinger equation with this configuration of bond potentials (i.e. by just one cycle of the iteration described above). The force caused by the strain within bond *i* acts on the two adjacent sites *i* and *i*+1 and is projected to the *x* axis by the angle  $\varphi_i$ . The strain within the two adjacent bonds *i*-1 and *i* contributes to the force acting on site *i*.

$$F_i = \begin{bmatrix} + (\tilde{\rho}_i - \rho_i) a \cos \varphi_i \\ - (\tilde{\rho}_{i-1} - \rho_{i-1}) a \cos \varphi_{i-1} \end{bmatrix} \cdot k a \quad (3)$$

Newton's equation (2) with the force (3) is approximated by a difference equation (Verlet algorithm) and is simplified to the equation (A7) describing the time evolution of the bond potentials. This is outlined in the Appendix.

The dynamical scaling factor *k* is thus the stiffness of the bond deviating from its equilibrium (this equilibrium itself depends on the electron-phonon coupling constant  $\alpha=1.95$ ). The value  $k = 11.2 \text{ eV \AA}^{-2}$  is obtained from scaling the time axis: calculating the frequency  $\nu_{\text{max}}$  of the in-phase-stretching-mode of the polyene lattice by numerical integration of (A7) and comparing it with the experimental value  $\nu_{\text{max}} = c \cdot 1400 \text{ cm}^{-1}$  (vibronic structure of the absorption band of polyenes). Thus starting with an appropriate initial condition and proceeding equation (A7) with time step  $\Delta t = 1.25 \cdot 10^{-15} \text{ sec}$  the time propagation of the non-linear excitation under consideration is obtained. The dynamical scaling factor *k* should not be confused with

the force constant  $K = \frac{(2\pi \nu_{\text{max}})^2 M_{\text{CH}}}{4 \cos^2 \varphi} = 31.5 \text{ eV \AA}^{-2}$

the  $\sigma$ -bond compressed by the  $\pi$ -electrons. The velocity of sound along *s* is  $v_s = 1.85 \cdot 10^4 \text{ m sec}^{-1}$ . Scaling the time axis not to  $\nu_{\text{max}}$  but to Raman data on benzene with  $K = 47.5 \text{ eV \AA}^{-2}$  the values  $\Delta t = 1.02 \cdot 10^{-15} \text{ sec}$ ,

$k = 16.9 \text{ eV \AA}^{-2}$ ,  $v_s = 2.27 \cdot 10^4 \text{ m sec}^{-1}$  are obtained. However, since *k* scales the time axis, the gap (which is defined by  $\alpha$ ) and thus the course of the dynamics is unaffected by this parameter. In contrast, treating the electron-phonon coupling within the (SSH)-model (parameters *K*,  $t_0$ ,  $\alpha_{\text{SSH}}$ ), the minimum of the total energy is determined. This leads to a serious inherent inconsistency: the value  $\lambda=0.2$  of the parameter

$$\lambda = \frac{2 \alpha_{\text{SSH}}^2}{\pi t_0 K}$$

fits the experimental value of the band gap,

but the value  $\lambda=0.08$  calculated from the experimental values of *K* and of the bond lengths of graphite and benzene (giving  $\alpha_{\text{SSH}}/K$ ) leads to a band gap smaller than the experimental value by a factor 1/40. This clear disagreement is usually assumed to be an indication of the failure of the single-particle picture and thought to be removed by explicitly taking electron-electron correlation into account [20]. However, there is no such inconsistency within the (NFE)-model [23].

### DYNAMICS OF THE NEUTRAL KINK

The time evolution of a neutral kink embedded in a ring with 139 sites initially at rest with velocity boosts (Fig. 3)

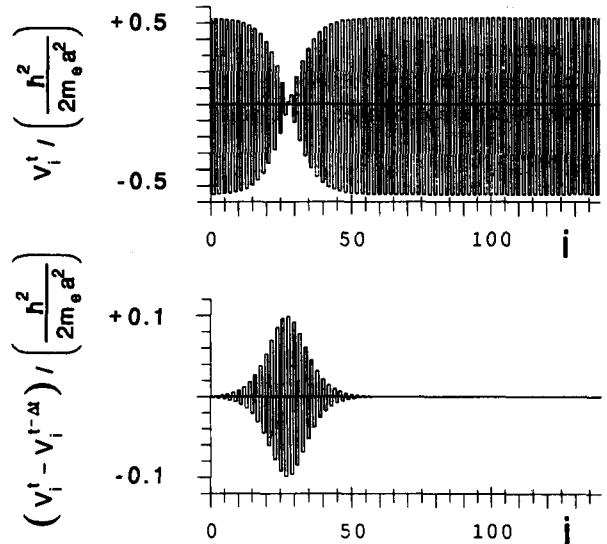
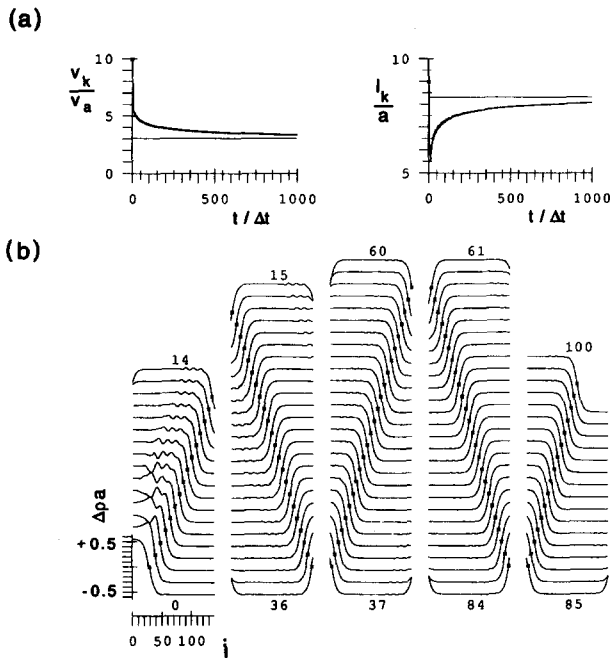


Fig.3 Initial condition for dynamics of the kink in Fig.4. Above, potential steps of alternating lower (higher) values correspond double (single) bonds. Defect located at *i*=27. Below, velocity boost for velocity  $\eta v_s$ ,  $\eta = 10$  obtained by  $V_i^t - V_i^{t-\Delta t} = \eta v_s \Delta t \frac{-\alpha}{2} (\rho_i - \rho_{i+2}) \cdot \frac{\hbar^2}{2ma^2}$ . (since solitons are degenerate if translated by  $2a$ ).



**Fig.4** Dynamics of a neutral kink along a ring of 139 sites (139 bonds) with an initial velocity  $v_k = 10 v_a$  during 1000 time steps of  $\Delta t = 1.25 \cdot 10^{-15}$  sec. a) Time evolution of the kink velocity  $v_k$  and kink width  $l_k$ . b) Time evolution of the charge density alternation  $\Delta \rho_i = (-1)^i (\rho_{i+1} - \rho_i)$ . Spot-light every  $10\Delta t$  indicated by numbers 0-100.  $\Delta r = 0$  indicated by star. To avoid kink-phonon collision, phonons evolving behind the fast moving kink are relaxed removing kinetic energy by

$V_i^{t+\Delta t} = V_i^t + \Delta t^2 \omega^2 \chi_i^t \cdot \frac{\hbar^2}{2ma^2}$  within the soliton-free region for each time step, until steady state of the moving kink is reached. During this procedure, where a section of the lattice is relaxed, the total energy is not conserved.

of  $v_k = 10 v_a$  [25] is investigated (Fig. 4). Immediately after the boost the velocity of the kink  $v_k$  drops down to  $v_k = 5 v_a$  as well as its width  $l_k$ , from initially  $l_k = 9 a$

to  $l_k = 6.5 a$  (Fig. 4a), while the rise of a huge hump behind the soliton takes over the excess kinetic energy. The hump starts to oscillate and smaller wiggles with frequency  $0.94 v_{\max}$  and wave length  $13 a$  develop behind the kink, slowing it down further and increasing its width again (Fig. 4b). The vibration is due to the fact that the soliton, as it moves over a distance given by its width produces a maximum in the alternation and leaves a minimum behind. With progressive time evolution the amplitude of these wiggles fades away and the soliton reaches a constant width of  $l_\infty = 8.3 a$  and a constant velocity of  $v_\infty = 3.05 v_a$  without energy dissipation into the lattice. Guinea [5] and Bishop et al. [4] obtain within the SSH-model  $v_\infty$  values between  $v_\infty = 0.6 v_a$  and  $v_\infty = 4.0 v_a$  by using different values of adjustable parameters. Waves of wavelength  $12 a$  were also described by Guinea [5] for  $v_k = 4.3 v_a$  and  $v_k = 3.0 v_a$ . Note that the result  $v_\infty = 3.05 v_a$  depends on the electron-phonon coupling  $\alpha$  scaled to experimental bond lengths, but not on the dynamical scaling factor  $k$ .

## CONCLUSIONS

The step potential model is the conceptually simplest approach to treat the electron-phonon coupling in  $\pi$ -electron systems and is the logical extension of the free electron model. Scaled to the experimental bond lengths of butadiene and benzene the static properties of nonlinear excitations in polyacetylene are well described. Based on standard adiabatic approximation the extension of the step potential model to study the dynamical behaviour of nonlinear excitations in polyacetylene is straightforward. The time is scaled to the frequency of the in-phase-stretching-mode of the polyene lattice. However, the course of the dynamics (i.e. maximum velocity of a neutral kink with regard to velocity of sound) is independent on the time scaling factor.

*Acknowledgements* - The authors are grateful to Profs. I. Kušćer and S.Roth for valuable discussions. The use of computer facilities at the ETHZ is acknowledged.

## REFERENCES

1. F.L.Carter, A.Schulz, D.Duckworth, in *Molecular Electronic Devices II*, F.L.Carter, Ed., M.Dekker, New York (1987)
2. S.Roth, H.Bleier, in *Molecular Electronics-Science and Technology*, A.Aviram, Ed., Engineering Foundation Conferences, New York (1989)
3. W.P.Su, J.R.Schrieffer, *Proc. Natl. Acad. Sci. USA* **77**, 5626 (1980)
4. A.R.Bishop, D.K.Campbell, P.S.Lomdahl, B.Horowitz, S.R.Phillpot, *Phys. Rev. Lett* **52**, 671 (1984)
5. F.Guinea, *Phys. Rev. B* **30**, 1884 (1984)
6. C.L.Wang, F.Martino, *Phys. Rev. B* **34**, 5540 (1986)
7. A.Terai, Y.Ono, *J. Phys. Soc. Jpn.* **55**, 213 (1986)
8. S.R.Phillpot, D.Baeriswyl, A.R.Bishop, P.S.Lomdahl, *Phys. Rev. B* **35**, 7533 (1987)
9. F.Chien, Y.Kashimori, K.Nishimoto and O.Tanimoto *Chem. Phys.* **125**, 269 (1988)

10. W.Förner, C.L.Wang, F.Martino, J.Ladik  
*Phys. Rev. B* **37**, 4567 (1988)
11. Y.Ono, A.Terai, *J. Phys. Soc. Jpn.* **59**, 2893 (1990)
12. C.Tric, *J. Chem. Phys.* **51**, 4778 (1969)
13. T.Kakitani, *Prog. Theor. Phys.* **51**, 656 (1974)
14. J.Baumgarte, *Comp. Methods Appl. Mech. Eng.* **1**, 1 (1972)
15. R.W.Hockney, J.W.Eastwood, in *Computer Simulation using Particles*, McGraw-Hill, New York (1981)
16. H.J.C.Berendsen, W.F.van Gunsteren, in *Molecular Dynamics Simulation of Statistical-Mechanical Systems*, Proceedings of the Enrico Fermi School, G.Ciccotti, W.G.Hoover Eds., North-Holland p.43 (1986)
17. C.Kuhn, *Phys. Rev. B* **40**, 7776 (1989)
18. C.Kuhn, *Synth. Met.* **57**, 4350 (1993)
19. C. Kuhn, in Proceedings of *Future directions of non-linear dynamics in physical and biological Systems*, Lyngby, Denmark, (23.July -1.Aug. 1992), Plenum Press
20. D.Baeriswyl, D.K.Campbell, S.Mazumdar, in *Conjugated Conducting Polymers*, H.G.Kiess Ed., Springer Series in Solid State Sciences **102**, Springer Verlag, Berlin Heidelberg, p.7 (1992)
21. H.-D.Försterling, W.Huber, H.Kuhn *Int. J. Quantum Chem.* **1**, 255 (1967)

22. H.-D.Försterling, W.Huber, H.Kuhn, H.H.Martin, A.Schweig, F.F.Seelig, W.Stratmann, in *Optische Anregung Organischer Systeme*", W.Foerst Ed., Verlag Chemie, Weinheim (1966), p.55
23. H.Kuhn, C.Kuhn, *Chem. Phys. Lett.* **204**, 206 (1993)
24. D.Baeriswyl, G.Harbeke, H. Kiess, W.Meyer, in *Electronic Properties of Polymers*, J.Mort, G.Pfister Eds., Wiley, New York (1982), Chap.7
25. With the velocity  $v_F = \frac{\hbar}{4ma} = 1.3 \cdot 10^6$  m sec<sup>-1</sup> of a  $\pi$ -electron at the Fermi surface the ratio  $v_a/v_F = 0.014$ . The localized  $\pi$ -electron corresponding to a kink is fast enough to fill the space given by its wave function before the defect leaves the region with a velocity of the order of  $v_a$  and the adiabatic approximation is expected to give correct results. The validity of the adiabatic approximation must be seriously questioned for kink velocities of  $\approx 10 v_a$  and it surely breaks down for velocities approaching  $v_F$
26. To avoid time derivatives of square root terms in going from equation (A2) to equation (A5) we use  $\gamma = 0$  and for compensation  $\beta = 19.4$  (instead of  $\beta = 19.9$ , see [17]). With these values the single and double bonds in butadiene are evaluated to 1.466 Å and 1.329 Å respectively (instead of 1.48 Å and 1.34 Å)

## APPENDIX

The dynamics of bond  $i$  is given by (A.2) subtracting (2) from (A.1)

$$M_{CH} \cdot \frac{d^2}{dt^2} x_{i+1} = F_{i+1} \quad (A.1)$$

$$M_{CH} \cdot \frac{d^2}{dt^2} (d_i \cos \varphi_i) = F_{i+1} - F_i \quad (A.2)$$

According to (2) the total momentum is conserved

$$\frac{d}{dt} \sum_i P_i = \frac{d}{dt} \sum_i M_{CH} \frac{dx_i}{dt} = \sum_i F_i = 0 \quad (A.3)$$

Using force field (3), equation (A.4) with  $\beta = 19.4$  [26]

$$V_i / \frac{\hbar^2}{2ma^2} = \beta \left( \frac{d_i}{a} - 1 \right) \quad (A.4)$$

equation (A.2) can be written as

$$\frac{d^2}{dt^2} (V_i \cos \varphi_i) = \frac{\beta k}{M_{CH}} \cdot \begin{bmatrix} + (\tilde{\rho}_{i+1} - \rho_{i+1}) a \cos \varphi_{i+1} \\ - 2(\tilde{\rho}_i - \rho_i) a \cos \varphi_i \\ + (\tilde{\rho}_{i-1} - \rho_{i-1}) a \cos \varphi_{i-1} \end{bmatrix} \cdot \frac{\hbar^2}{2ma^2} \quad (A.5)$$

The  $\varphi_i$  are in the limits of  $28^\circ$  to  $32^\circ$ , thus they are all set time and space independent and equation (A.5)

$$\text{with } \omega^2 = \frac{\beta k}{M_{CH}} \quad \text{and} \quad \chi_i^t = \begin{bmatrix} + (\tilde{\rho}_{i+1} - \rho_{i+1}) a \\ - 2(\tilde{\rho}_i - \rho_i) a \\ + (\tilde{\rho}_{i-1} - \rho_{i-1}) a \end{bmatrix}$$

is simplified to

$$\frac{d^2}{dt^2} V_i = \omega^2 \chi_i^t \cdot \frac{\hbar^2}{2ma^2} \quad (A.6)$$

To integrate equation (A.6) we use its discrete form

$$V_i^{t+\Delta t} = 2V_i^t - V_i^{t-\Delta t} + (\Delta t \omega)^2 \chi_i^t \cdot \frac{\hbar^2}{2ma^2} \quad (A.7)$$

With  $\Delta t \omega = 0.5$  we have chosen a time step

$\Delta t = \frac{1}{19.1 v_{\max}}$  sufficiently small to reach good accuracy and stability [16]. The conservation of the total energy is proved by demonstrating constant velocity of a kink moving with low speed, i.e. below its maximum velocity.